The Journal of Experimental Biology 202, 333–345 (1999)
Printed in Great Britain © The Company of Biologists Limited 1999
JEB2530

THE INFLUENCE OF TEMPERATURE ON POWER PRODUCTION DURING SWIMMING

II. MECHANICS OF RED MUSCLE FIBRES *IN VIVO*

LAWRENCE C. ROME[1,3,*], DOUGLAS M. SWANK[2,3,‡] AND DAVID J. COUGHLIN[1,3,§]

[1]*Department of Biology and* [2]*Department of Physiology, University of Pennsylvania, Philadelphia, PA 19104, USA* and [3]*Marine Biological Laboratories, Woods Hole, MA 02543, USA*

*e-mail: lrome@mail.sas.upenn.edu

‡Present address: Department of Biology, San Diego State University, San Diego, CA 92182, USA

§Present address: Science Division, Widener University, One University Place, Chester, PA 19013, USA

Accepted 14 September; published on WWW 22 December 1999

Summary

We found previously that scup (*Stenotomus chrysops*) reduce neither their stimulation duration nor their tail-beat frequency to compensate for the slow relaxation rates of their muscles at low swimming temperatures. To assess the impact of this 'lack of compensation' on power generation during swimming, we drove red muscle bundles under their *in vivo* conditions and measured the resulting power output. Although these *in vivo* conditions were near the optimal conditions for much of the muscle at 20 °C, they were far from optimal at 10 °C. Accordingly, *in vivo* power output was extremely low at 10 °C. Although at 30 cm s^{-1}, muscles from all regions of the fish generated positive work, at 40 and 50 cm s^{-1}, only the POST region (70 % total length) generated positive work, and that level was low. This led to a Q_{10} of 4–14 in the POST region (depending on swimming speed), and extremely high or indeterminate Q_{10} values (if power at 10 °C is zero or negative, Q_{10} is indeterminate) for the other regions while swimming at 40 or 50 cm s^{-1}.

To assess whether errors in measurement of the *in vivo* conditions could cause artificially reduced power measurements at 10 °C, we drove muscle bundles through a series of conditions in which the stimulation duration was shortened and other parameters were made closer to optimal. This sensitivity analysis revealed that the low power output could not be explained by realistic levels of systematic or random error. By integrating the muscle power output over the fish's mass and comparing it with power requirements for swimming, we conclude that, although the fish could swim at 30 cm s^{-1} with the red muscle alone, it is very unlikely that it could do so at 40 and 50 cm s^{-1}, thus raising the question of how the fish powers swimming at these speeds. By integrating *in vivo* pink muscle power output along the length of the fish, we obtained the surprising finding that, at 50 cm s^{-1}, the pink muscle (despite having one-third the mass) contributes six times more power to swimming than does the red muscle. Thus, in scup, pink muscle is crucial for powering swimming at low temperatures.

This overall analysis shows that Q_{10} values determined in experiments on isolated tissue under arbitrarily selected conditions can be very different from Q_{10} values *in vivo*, and therefore that predicting whole-animal performance from these isolated tissue experiments may lead to qualitatively incorrect conclusions. To make a meaningful assessment of the effects of temperature on muscle and locomotory performance, muscle performance must be studied under the conditions at which the muscle operates *in vivo*.

Key words: muscle function, scup, *Stenotomus chrysops*, mechanical power, muscle mechanics, work loop, temperature effect.

Introduction

The power that muscle generates depends on the length change and stimulation pattern that the muscle undergoes as well as its contractile properties (Josephson, 1985; Josephson and Stokes, 1989; Marsh, 1990; Altringham and Johnston, 1990; Marsh et al., 1992; Rome et al., 1993). As discussed in the preceding report (Swank and Rome, 1999), it appears that the more closely the length change and stimulation pattern through which the red muscle is driven follow the *in vivo* pattern, the more power output is reduced at low temperatures, thus raising the Q_{10} for power production. For instance, if scup (*Stenotomus chrysops*) red muscle is stimulated with a duty cycle of 42 % (the approximate *in vivo* duty cycle for the ANT-2 position at 40 % total length of the fish) and is driven with an oscillatory length change at 4–5 Hz (equivalent to tail-beat frequency at 50 cm s^{-1}), it generates very little power at 10 °C, but high power at 20 °C (Rome and Swank, 1992). Thus, even

though in this experiment the strain and phase were optimized to improve power, the resulting Q_{10} for power production is very large (approximately 10). These results show that the Q_{10} of power production *in vivo* can be much larger than that predicted from force–velocity curves (1.8; Rome et al., 1992b) or from typical 'optimized' work-loop experiments (2.3; Rome and Swank, 1992). Further, the Q_{10} may become even larger when the strain and phase are no longer optimized, but are adjusted to their *in vivo* values. Accordingly, these findings raise the question: how do fish power steady swimming at low temperatures if their muscles generate so little power?

The lower power output of cold muscles is principally due to their slower relaxation rates. Hence, oscillatory power output at low temperatures can be increased by reducing stimulation duration or by reducing oscillation frequency. In the preceding report (Swank and Rome, 1999), we observed no such compensatory changes in the *in vivo* length change and stimulation pattern; electromyogram (EMG) duty cycle at any position along the length of the fish and muscle oscillation frequency were essentially independent of temperature. However, we did observe that, moving caudally, the stimulus duty cycle decreases to well below the value of 42 % used by Rome and Swank (1992), which might improve power generation in these regions. Further, it has also been found that the contractile properties of scup red muscle vary along the length of the fish: moving anteriorly, muscle has a faster relaxation rate (Rome et al., 1993; Swank et al., 1997), which might aid in power generation in the anterior of the fish at low temperatures.

To determine how the position-dependencies of the contractile properties and the *in vivo* length change and stimulation pattern interact to set power production along the length of the fish, we drove muscles from each position through their *in vivo* length change and stimulus pattern, and measured force and power production. From this analysis, we hope to gain greater insight into how temperature affects *in vivo* muscle function and how muscles power swimming at different temperatures.

Materials and methods

Fish

Scup (*Stenotomus chrysops* L.) were caught by hook and line in Woods Hole, MA, USA, and acclimated for 6 weeks to 20 °C. Thus, in these experiments, we examined the effects of acute changes in temperature. Fish, matched in length with those in Swank and Rome (1999) (20–25 cm), were killed with a blow to the head and double-pithed.

Mechanics experiments

Bundles of red muscle fibres were dissected from four regions of the fish: ANT-1 (29 % of the distance from snout to tail), ANT-2 (40 %), MID (54 %) and POST (70 %). Each bundle was tied to a force transducer and a servomotor and stimulated through platinum plate electrodes. A force–length curve was then obtained for the bundle. The initial length for the work-loop experiments was set on the plateau of this curve where a 5 % length change would cause a similar decrement in active force at both the shortest and longest lengths (as in Rome and Swank, 1992). On the basis of previous histological studies (Rome et al., 1992a), this corresponded to an initial sarcomere length of 2.1–2.2 μm.

The appropriate *in vivo* length change and stimulation patterns were imposed on bundles from each region of the fish using computer control (as in Rome and Swank, 1992; Rome et al., 1993). Spectrum analysis of the length change recording of the MID and POST regions (Swank and Rome, 1999) showed that they contained higher-frequency components in addition to the fundamental frequency and were slightly better fitted by a triangular wave than by a sinusoid. We therefore drove the muscle using a triangular wave in which the sharp corners were digitally rounded. As such, this waveform represents a compromise between a pure sinusoid and pure triangular wave. As we were unable to observe higher-frequency components in the length changes of the ANT-1 and ANT-2 positions, their length change was approximated by a sinusoidal waveform.

The work generated by the muscle during the shortening/lengthening cycles was calculated using custom-designed software (Rome and Swank, 1992). Muscle volume was approximated by photographing the bundle from the side (bundle thickness and bundle length) and from the top (bundle width). Because of the large amount of connective tissue and fat in the bundle, on the basis of previous histological studies, we calculated the cross section (and volume) occupied by muscle fibres as 43 % of the overall cross section (Rome and Sosnicki, 1990; Rome et al., 1992b). Bundle mass was obtained assuming a density of $1.06\,g\,cm^{-3}$.

Preliminary experiments showed that maximum power output was reached in relatively few oscillation cycles when the muscle was run at near-optimal stimulation and length-change conditions. However, the further the imposed conditions were from these optimal conditions (see Fig. 6), the more cycles were necessary to achieve a leveling of power output (note that work *increased* with cycle number until it plateaued). For instance, under POST conditions at 20 °C (short stimulation duration, long strain), power output leveled off within approximately eight cycles. Under ANT-1 conditions at 20 °C (long stimulation duration, short strain), it took approximately 20 cycles for the power to plateau. At 10 °C, ANT-1 conditions are much further from optimal than at 20 °C. Hence, muscles had to be run through approximately 50 cycles prior to the work production leveling off.

Our rationale for waiting until power levelled off, rather than examining power at a fixed cycle number under all conditions, is that the red muscle is used during steady swimming and, thus, for thousands of consecutive tail beats (scup will readily swim for over 5 h with a 4–5 Hz tail-beat frequency, which requires in excess of 80 000 tail beats). Hence, if it takes some time to achieve a steady state naturally, or if the manner in which we are stimulating requires time to reach a steady state, then it seemed reasonable to wait rather than to take a value

after an arbitrary time. In addition, it should be recognized that this large number of cycles is not due to the poor quality of the preparation. Running the same muscle under a set of optimal conditions even at 10 °C permits the muscle to reach its steady state in under 10 cycles, typical of other muscles on which optimized work-loop experiments have been performed (Altringham et al., 1993).

Because different numbers of cycles had to be performed under different conditions, the time allowed for the muscle to rest between trials varied between 5 min (at 20 °C under near-optimal conditions) and 30 min (at 10 °C under non-optimal conditions). This fact greatly influenced the amount of data that could be obtained from a single preparation. At 20 °C, a muscle from one region of the fish could be run through all the *in vivo* length change and stimulation conditions it would encounter at different speeds, as well as the conditions encountered at other positions of the fish (see Results). At 10 °C, however, it was possible to obtain data from only three sets of *in vivo* conditions. These corresponded to the *in vivo* conditions that a muscle from a particular region of the fish would encounter at 30, 40 and 50 cm s^{-1}.

In addition to being run under the *in vivo* conditions, the stimulation and length-change conditions for each muscle bundle were optimized to determine the maximum power the bundle could generate (Josephson, 1985; Altringham and Johnston, 1990; Rome and Swank, 1992; Davies and Johnston, 1995). This was performed for two reasons. First, all the data could then be expressed as a proportion of this maximum power. We could therefore differentiate between variance in maximum power generation and variance in the proportion of maximum power generated under *in vivo* conditions. The expectation was that the variance in the proportion of maximum power generated under a particular set of *in vivo* conditions would be smaller than the variance in maximum power per kilogram (which also depends on the accuracy with which the muscle volume was determined). Second, maximum power generation was used as a measure of muscle deterioration. Thus, maximum power was determined at regular intervals. The frequency of the measurements was sufficiently often that maximum power did not fall by more than 2–3 % between each measurement. It should be noted that this value is more useful than monitoring only isometric force, because determination of maximum power integrates the muscle's ability to activate, generate force, shorten and relax, and thus would be sensitive to decrements in any one of the components involved.

We also measured the maximum power that the muscle could generate at the frequencies corresponding to the tail-beat frequencies found under the *in vivo* conditions (FREQMAX). This involved optimizing the strain, stimulation duration and stimulation phase for maximum power generation at that frequency. Knowing the maximum power that could be achieved at the frequency in question, one could determine how far power generation was from this maximum when the muscle was working under *in vivo* conditions. In addition, by determining the optimal length change and stimulation conditions at this frequency, we could ascertain how far from optimal the measured *in vivo* conditions were. This is crucial information for performing a sensitivity analysis (see Results).

At 20 °C, muscle was studied at conditions corresponding to a swimming speed of 80 cm s^{-1} (oscillation frequency 6.4 Hz) (some of these data were reported previously by Rome et al., 1993) and 50 cm s^{-1} (oscillation frequency 4.68 Hz). At 10 °C, muscle was studied at conditions corresponding to 50 cm s^{-1} (oscillation frequency 4 Hz) and 30 cm s^{-1} (oscillation frequency 2.85 Hz).

To minimize fatigue of the muscle, the lower *in vivo* frequency at each temperature (4.68 Hz at 20 °C and 2.85 Hz at 10 °C) was taken to represent the oscillation frequency at which maximum power is generated at the respective temperatures. We had previously found that 5 Hz and 2.5 Hz were the approximate oscillation frequencies for the power maximum at 20 °C and 10 °C, respectively (Rome and Swank, 1992), and that the power *versus* frequency curve was quite broad. Hence, using these frequencies gave us a close approximation to maximum power generation.

Statistics

Statistical analyses were performed using SigmaStat software (Jandel). To compare means, *t*-tests were typically used, and analysis of variance (ANOVA) was used in some cases. Statistical significance was set at $P<0.05$.

Results

Relaxation rate varied both along the length of the fish and with temperature (Figs 1, 2). We have previously shown that, at 20 °C, relaxation rate varies considerably along the length of the fish, becoming faster anteriorly (Rome et al., 1993; Swank et al., 1997). The same trend is observed at 10 °C, with the absolute time differences being even more dramatic (Figs 1, 2). The temperature effect (Q_{10}) for muscle relaxation appears to be greater in the anterior (3.6) than the posterior (2.8), but this was not statistically different (ANOVA, $P=0.134$). The rate of activation was independent of position and had a somewhat smaller Q_{10} (approximately 2.1) than for relaxation (*t*-test, $P<0.001$) (Figs 1, 2). Isometric force was essentially independent of position, and the Q_{10} has a modest value (1.19±0.06, mean ± S.E.M., $N=28$, averaged for all positions; Fig. 3).

Because of the slower relaxation rate, slower activation and lower maximum shortening velocity, V_{max}, maximum oscillatory power was considerably lower at 10 °C than at 20 °C, and the frequency for maximum power output (f_{opt}) was shifted to a lower value (approximately 2.5 Hz *versus* 5 Hz as found previously by Rome and Swank, 1992). At the top swimming speed prior to white muscle recruitment, red muscle was used at higher frequencies *in vivo* than that at which maximum power is obtained in *optimized* work-loop experiments on isolated muscle. This departure was more marked at 10 °C than 20 °C (i.e. 1.6 times higher frequency at 10 °C and 1.28 times higher

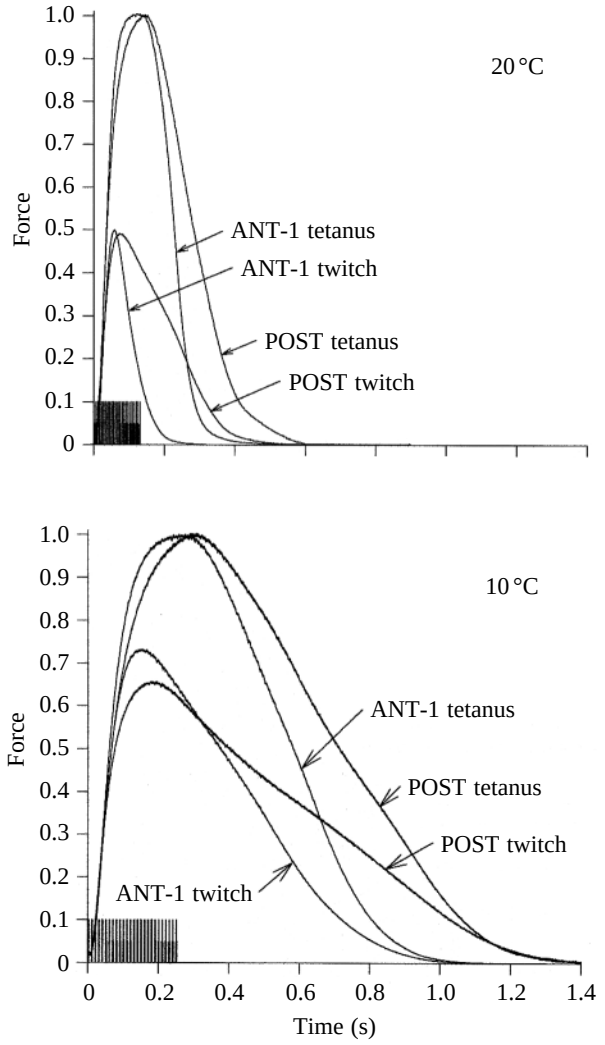

Fig. 1. Tetanus and twitch force recordings at 10 °C and 20 °C from ANT-1 and POST muscle bundles. For each bundle, the forces are normalized to peak tetanic tension. The timing of stimuli for the tetani are shown by multiple vertical lines (duration 130 ms at 20 °C and 250 ms at 10 °C). The relaxation rate was much slower at 10 °C than 20 °C, and the POST muscle relaxation rate was slower than that of the ANT-1 muscle bundle.

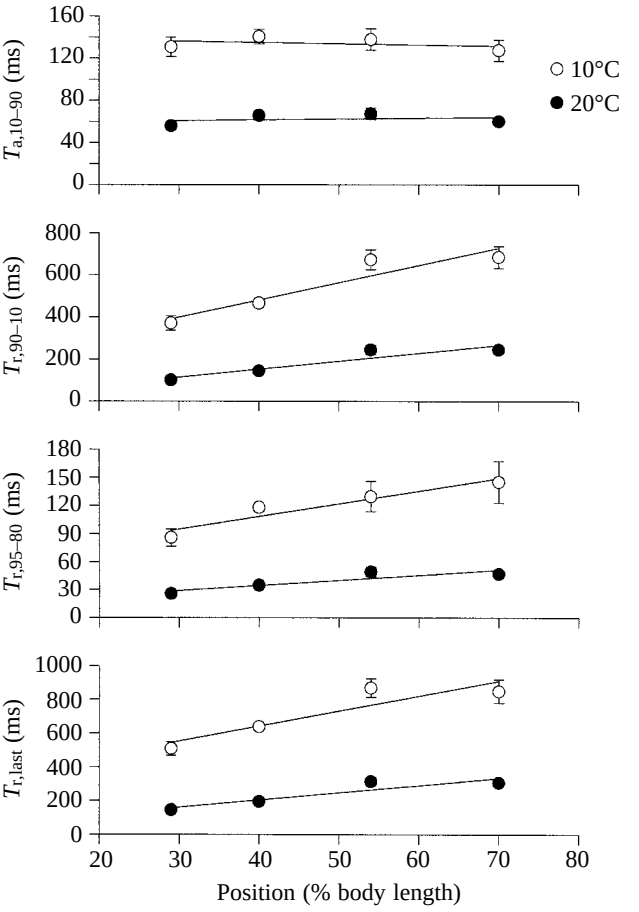

Fig. 2. Activation and relaxation times plotted *versus* body position from which the muscle bundle was removed. Although there was no difference in activation time with position (one-way ANOVA, P=0.865 for 10 °C, P=0.557 for 20 °C), relaxation time slows dramatically moving posteriorly along the fish (one-way ANOVA, P<0.038 for all variables except $T_{r,95–80}$ at 10 °C, where P=0.391). The MID muscle tends to have a slightly slower relaxation rate than the POST muscle, but this was not statistically significant (Tukey multiple-comparison test, P>0.05 for all three measurements). Activation time was the time it took for the force to increase from 10 % to 90 % of maximum force ($T_{a,10–90}$); relaxation time was measured in three ways: the time needed to relax from 90 % to 10 % of maximum force ($T_{r,90–10}$), the time needed to relax from 95 % to 80 % of maximum force ($T_{r,95–80}$), and the time between the last stimulus and the point where tension fell to 10 % of maximum force ($T_{r,last}$). Values are mean ± S.E.M., N=5–7.

at 20 °C). Maximum power output averaged over all positions was 11.5±1.0 W kg^{-1} (N=28) at 10 °C *versus* 31.0±2.7 W kg^{-1} (N=17) at 20 °C. Optimized oscillatory power for the ANT-1 position at 20 °C tended to be somewhat higher than in other positions, but this was not statistically significant (Fig. 3).

The slower relaxation rate of red muscle at 10 °C had additional important consequences for power-generating capabilities under *in vivo* conditions. Because of its slower relaxation rate, for muscle to generate its maximum power at 10 °C, it must be driven at a slower oscillation frequency and with a shorter stimulus duty cycle than at 20 °C (Rome and Swank, 1992). However, as shown by Swank and Rome (1999), neither of these changes occur *in vivo* at 10 °C; EMG durations are nearly the same as at 20 °C, and tail-beat frequency is reduced by only a small amount, if at all. This results in very low *in vivo* power generation at 10 °C.

At 10 °C under 30 cm s^{-1} *in vivo* conditions (oscillation frequency 2.85 Hz), on average the red muscle generates positive work in all regions of the fish (Figs 4, 5; note that some individual ANT-2 bundles generated negative work). However, under 50 cm s^{-1} *in vivo* conditions (oscillation frequency 4.0 Hz), positive work was generated only in the POST region of the fish. Thus, at speeds greater than 30 cm s^{-1}, only the POST muscle generated positive work (see Fig. 5 and

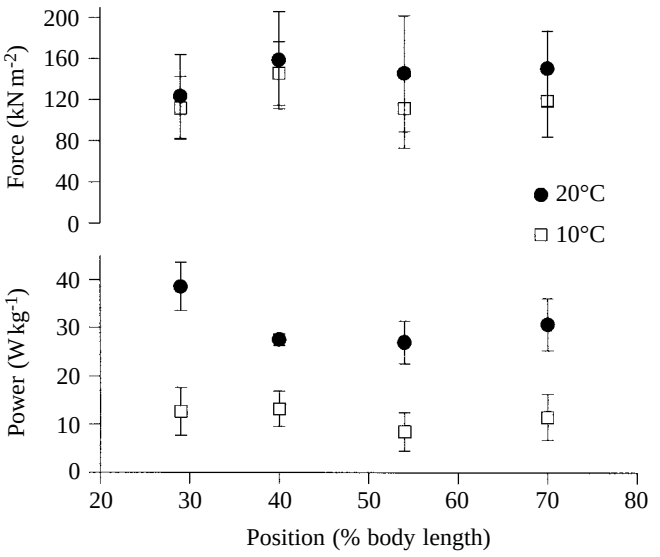

Fig. 3. Force and maximum oscillatory power output as a function of position and temperature. Maximum isometric force was independent of muscle position (one-way ANOVA, P=0.993 for 10 °C and P=0.970 for 20 °C) and was modestly temperature-dependent (mean Q_{10}=1.19). Maximum power (measured under 'optimized' conditions) was very temperature-dependent. At 20 °C, bundles from the ANT-1 position (30 % along the length of the body) tended to generate higher power than those from the other positions, but this was not statistically significant (one-way ANOVA, P=0.577 for 20 °C, P=0.894 for 10 °C). Values are mean ± S.E.M., N=5–8.

Discussion). This is in dramatic contrast to the situation at 20 °C, where positive power is generated at every position. Thus, the Q_{10} for *in vivo* power output of the POST muscle ranged from 4 to 14 depending on the swimming speed examined.

Low power output at cold temperatures: sub-optimal conditions

To determine whether the low power generation at 10 °C was primarily due to the high (compared with f_{opt}) *in vivo* oscillation frequency at which the muscle operated *versus* the actual *in vivo* strain and stimulation conditions it was being driven through, we determined the optimal length change and stimulation conditions for power production at each of the frequencies studied. Figs 4 and 5 show that, even at the highest frequency at 10 °C (4 Hz), the muscle is capable of generating far greater power (FREQMAX) than under the *in vivo* conditions. Thus, the suboptimal nature of the *in vivo* strain and stimulation conditions are what cause low power production, not the high oscillation frequency *per se*. As shown in Fig. 6, there can be large deviation between *in vivo* and optimal conditions. In particular, the stimulation duty cycle in the swimming fish is generally much longer than the optimal values, and the strain in the swimming fish is generally shorter than the optimal value. Further, this deviation is far more dramatic in the anterior *versus* posterior regions, and the deviation of stimulus duty cycle from optimal is far greater at the lower temperature. Also at 10 °C, the deviation increased with higher swimming speeds (higher tail-beat frequency). Thus, the long stimulus duty cycle in combination with the short strain resulted in negative work generation at ANT-1, ANT-2 and MID position at swimming speeds above 30 cm s^{-1} at 10 °C. This causes the Q_{10} measured under *in vivo* conditions at 50 cm s^{-1} to be very large and essentially indeterminate for the ANT-1, ANT-2 and MID regions, at which net power output at 10 °C is negative. The POST muscle is able to generate work at 50 cm s^{-1} because the relatively long strain and short duty cycle it undergoes are closer to optimal than in the other regions of the fish.

Sensitivity analysis: could errors in the in vivo *measurements cause low power values at 10 °C?*

On the basis of the extraordinarily low power generated by red muscle at 10 °C when the fish swims at 50 cm s^{-1} (Figs 3, 4), it seemed doubtful that the red muscle would be able to power swimming at this speed. Yet we know that fish swim at these speeds at 10 °C without using their white muscle (Swank and Rome, 1999). The possibility arises that the muscle at 10 °C may be extremely sensitive to stimulus and length-change conditions, and that *small* systematic or random errors in our measurements of these *in vivo* parameters could cause *large* non-linear differences in power output of the isolated muscle bundles, and thus qualitatively alter the picture. We performed additional experiments to try to assess this possibility.

It is clear that the muscle can generate considerable power at 10 °C if the stimulation duration, strain and phase are optimized at each oscillation frequency (tail-beat frequency; see FREQMAX in Figs 4, 5). Could measurement errors in our *in vivo* length change and stimulation conditions cause artificially low power measurements? One potential source of error is EMG duration. As mentioned by Swank and Rome (1999), computerized measurements of rectified EMGs do give somewhat shorter duty cycles, because they do not include slowly varying voltages that may represent motion artefacts. Clearly, the *in vivo* stimulation duty cycle is far longer than those obtained during optimized conditions (Fig. 6), and a shorter stimulus duty cycle might improve power production. In addition, strain has an effect on power output. Our procedure of digitally filtering the length change data so that it could be fitted with a spline to determine more accurately the length maximum for the calculation of phase could, in theory, lead to a slight underestimation of strain. In addition, the poor signal-to-noise ratio in the anterior region of the fish could, in theory, result in further underestimation of strain. If power production were extremely sensitive to the value of strain, then small errors in these measurements could also cause a large effect.

To test these possibilities, we drove muscle bundles though a series of conditions in which the stimulus duty cycle was shortened, the strain increased and the phase shifted to more negative values (i.e. closer to optimal work-loop conditions). Because of the difficulty in running muscles at low temperatures through a large variety of conditions, each muscle

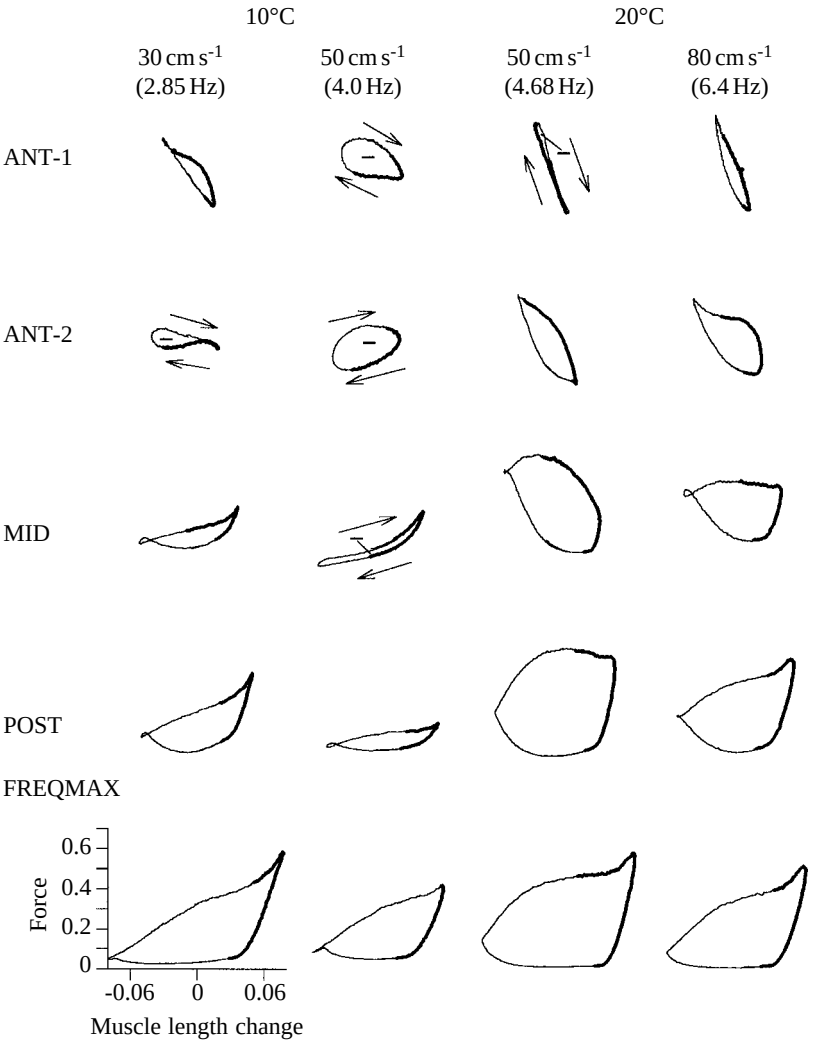

Fig. 4. Representative work loops for all *in vivo* conditions. The first four rows of each column show the work loops generated by a red muscle bundle from each position when driven under four sets of *in vivo* conditions (as measured in Swank and Rome, 1999). The 80 cm s^{-1} data at 20 °C are from Rome et al. (1993). The bottom row (FREQMAX) shows work loops generated when muscle length change, stimulus duration and phase were optimized to generate maximum power at the stated *in vivo* oscillation frequency and temperature. The timing of the stimulus relative to the total length change cycle is represented by the thickening of the loop. Loops denoted by a negative sign generated net negative work and progressed in a clockwise direction, whereas unmarked loops generated net positive work and progressed in an anti-clockwise direction. Force was normalized to isometric force at 20 °C. The *x*- and *y*-axes in the bottom left-hand graph represent scale bars for all the work loops. The muscle used for the bottom row (FREQMAX) was an ANT-1 bundle. Hence, the low work output at 10 °C is not due to an inability of the muscle to generate power but to the *in vivo* conditions.

at 10 °C was run through a limited set of conditions. Overall, we found that power output was reasonably insensitive to the small changes in the *in vivo* parameters that might reasonably occur as a result of error. For instance, at 10 °C, increasing the strain by 25 % over the measured value had little effect on power production (Table 1, long strain at each speed) and, importantly, did not change negative power values to positive. In addition, Fig. 7 shows that, at 20 °C, power output is changed relatively little by increasing the strain the muscle undergoes by 1 % of resting muscle length (POST LONG, ANT-1 LONG). The effect represents only an approximately 10 % increase in power output between POST LONG and POST conditions, where the change in strain is a small fraction (approximately 20 %) of the total length change. This power difference is even smaller between the ANT-1 and ANT-1 LONG conditions, where the difference in length change is quite substantial (approximately 40 %). Thus, under these *in vivo* conditions, small differences in muscle length change cannot cause large changes in power production.

Similarly, using shorter stimulus durations at 10 °C did not result in significant increases in power output (Table 1, manual selections at each speed). It should be noted that a manual analysis of the rectified EMGs (open triangles, Fig. 6) gave either the same or slightly shorter EMG durations than the computer analysis (open squares, Fig. 6); thus, these values were used for the sensitivity analysis. We also examined how small negative shifts in phase (approximately 15 °; i.e. the stimulus preceded shortening by a longer period) affected power. Although there were small improvements, again this did not lead to a major improvement in power production (Table 1, phase early at each speed).

Finally, one stimulus parameter that was not measured is the stimulus frequency within the envelope set by the EMG onset and offset. At 10 °C, we found that 100 pulses s^{-1} gave a fused tetanus, and thus a constant stimulation of 100 pulses s^{-1} was used. There was a possibility that the slow relaxation rate (and thus low power output) might be associated with a larger than normal Ca^{2+} release (compared with sarcoplasmic reticulum pump capacity) caused by an unphysiologically high stimulation frequency. Thus, we tried lower stimulation rates of 50 and 57 pulses s^{-1}. This did not increase power either (Table 1, stimulation frequency at each speed). Thus, although we cannot exclude the possibility that some unknown differences between stimulation by the nervous system *in vivo*

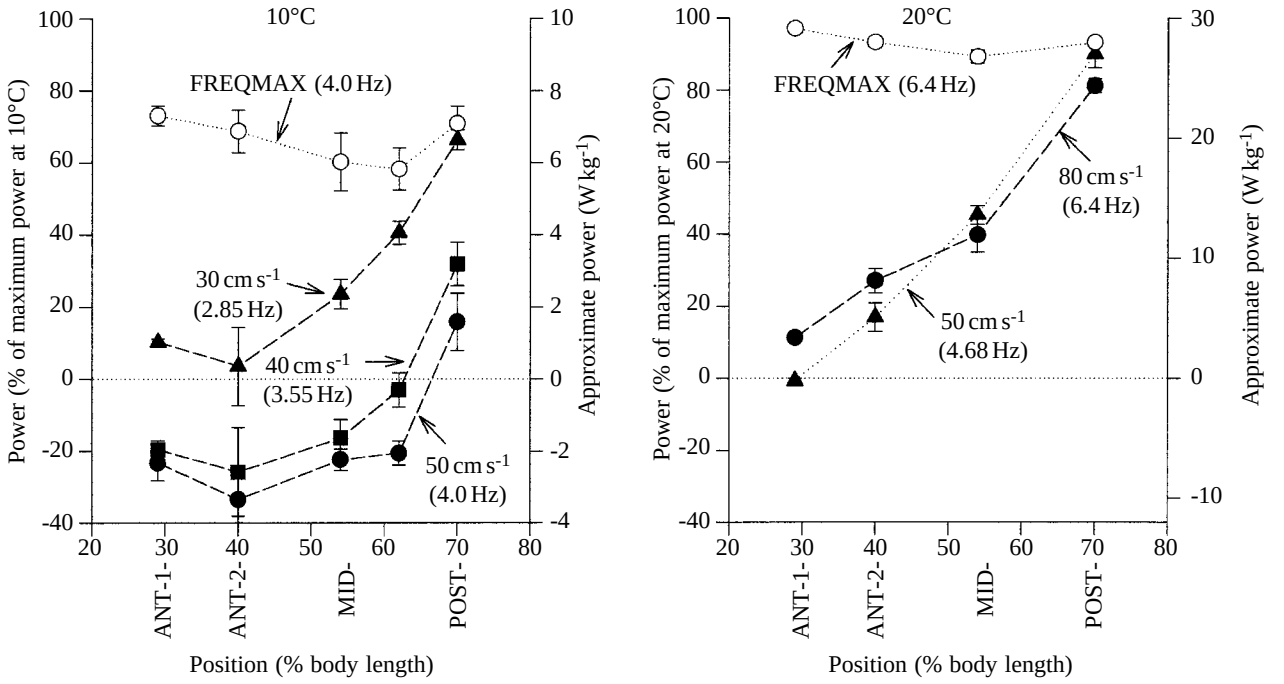

Fig. 5. *In vivo* power generated by muscle bundles from different positions along the fish at different swimming speeds and temperatures. Note that power is extremely dependent on position and is generally far smaller than the maximum power that the muscle could generate at the stated *in vivo* oscillation frequency (FREQMAX) except in the POST position at certain speeds. Power is expressed as a percentage of the maximum power-generating ability of the muscle at the experimental temperature (left-hand *y*-axis). The right-hand *y*-axis shows the approximate absolute power generated by the muscles expressed in W kg^{-1} (note the difference in scale at 10 °C compared with 20 °C). Note also that the absolute power scale is only approximate because values at each temperature are normalized for maximum power averaged over all the positions. Data at 80 cm s^{-1} at 20 °C are from Rome et al. (1993). Values are means ± S.E.M., *N*=5–8.

and our method of stimulation of the isolated muscle bundle may affect power production, these results suggest that high stimulation frequency alone was probably not responsible for the low power generation.

We conclude, therefore, that, even after accounting for reasonable levels of uncertainty associated with measurements of strain, EMG duration, phase and stimulation frequency, the mechanical power production patterns shown in Figs 4 and 5 are accurate.

Power generation by the red muscle at 10 °C

Having tried to exclude the possibility of systematic or random errors in measurements of the *in vivo* conditions as the cause of the strikingly low power output of the muscles at 50 cm s^{-1} at 10 °C, it seemed sensible to try to obtain additional information on red muscle power generation as a function of position and swimming speed to assess better how fish power swimming at low temperatures. Because there was such a large increase in power output during *in vivo* conditions between the MID and POST positions (Fig. 5), we obtained data at an intermediate position on the fish. At the midpoint between the MID and POST positions, we assumed that the *in vivo* parameters were intermediate between those of the MID and POST. Power production was found to be intermediate between the conditions, but generally closer to the MID value (Fig. 5A). Hence, very little, if any, additional power would be generated by the red muscle lying anterior to the POST position at 50 cm s^{-1}.

As there was also a very large reduction in power output between 30 cm s^{-1} and 50 cm s^{-1}, we also examined muscle power output at conditions corresponding to an intermediate speed (40 cm s^{-1}). The oscillation frequency (tail-beat frequency) was measured directly (3.55 Hz), and the other *in vivo* parameters (strain, duty cycle and phase) for that speed could be accurately interpolated from 30 and 50 cm s^{-1} data because the strain, stimulation duration and phase changed only slowly with swimming speed (Fig. 4 in Swank and Rome, 1999). As Fig. 5A shows, although power output was larger (i.e. less negative at 40 cm s^{-1} than at 50 cm s^{-1}), it was still negative at all positions except for POST.

Power output: contractile properties versus in vivo *conditions*

It is clear that the *in vivo* conditions become closer to the optimal for power production as one moves more posteriorly (Fig. 6). This is principally due to increased strain and decreased duty cycle. At the same time, however, contractile properties change in the opposite direction. Although activation rate and V_{max} are independent of position (Swank et al., 1997), relaxation rate slows as one moves caudally (Figs 1, 2). Thus, for a *given* set of stimulation and length-change conditions, power output would tend to be lower from bundles in the posterior half of the fish. To ascertain the relative effects of length-change and

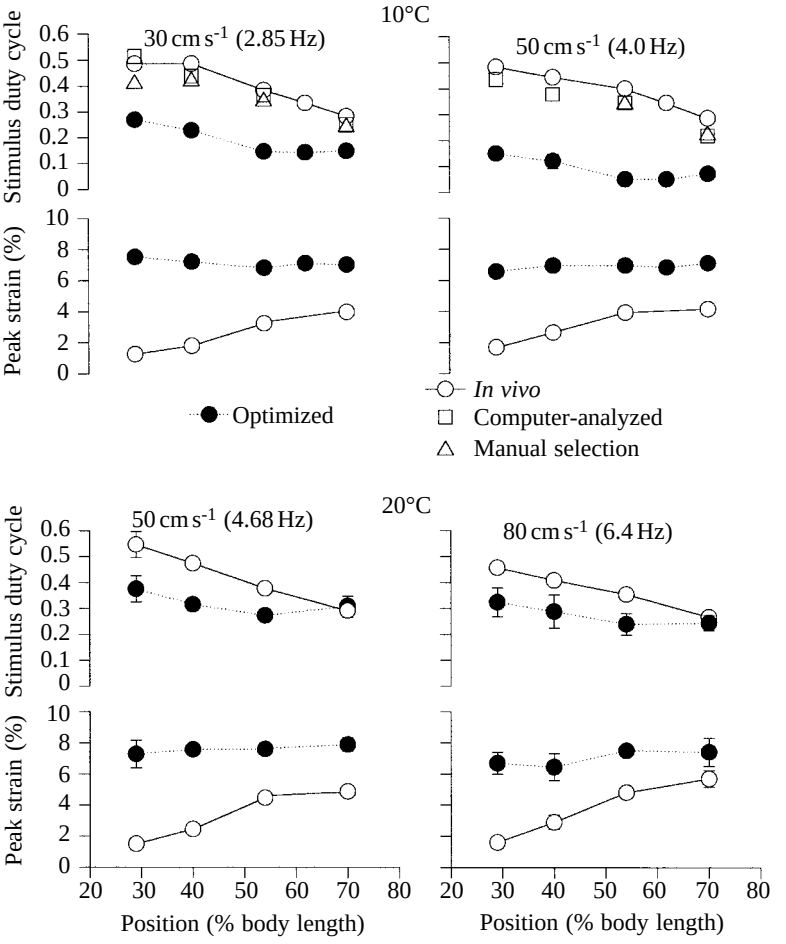

Fig. 6. Comparison of stimulus duty cycle and strain values that maximize power ('optimized'; filled symbols, dotted lines) with values measured *in vivo* (open symbols, solid lines). The difference was greatest at the anterior positions and at 10 °C. In addition, at 10 °C, increased swimming speed led to a greater difference between optimal and *in vivo* conditions (*t*-test on difference of means, $P<0.001$). Results from manual analysis of electromyogram (EMG) duration (circles) are shown for all temperatures and speeds. The results of two additional methods of measuring duty cycle are compared at 10 °C. For computer-analyzed duty cycles (squares), the trace was first rectified, a derivative taken, a threshold chosen (typically 12 μV) and a software subroutine automatically determined the onset and offset times. Similarly for manual selection (triangles), the EMG traces were rectified and a derivative taken, but the onset and offset times were determined by eye. These values were equal to or shorter than the others and were subsequently used in the sensitivity analysis. Values are means ± S.E.M., N=5–7.

stimulation parameters *versus* contractile properties along the length of the fish in setting power production, it was useful to drive muscles from each of the four positions (with their different contractile properties) through all the different length-change and stimulation conditions that muscles in the other regions undergo *in vivo*. This makes for a complicated matrix of contractions and, because of the large number of conditions necessary, it could only be performed at 20 °C: at 10 °C, the muscle needed a 30 min rest between each condition, making it impractical to impose a large series of conditions.

The experiments showed that muscle bundles from each of the positions generated the most power when driven under the POST conditions and generated the least power when driven under ANT-1 conditions (Fig. 7). We also found that, for every set of *in vivo* conditions, the ANT-1 muscle generally generated a greater percentage of maximum power than more posteriorly situated muscle (Tukey multiple-comparison test, $P<0.05$). This difference was relatively small for the POST conditions, which were nearly optimal for power generation, but became larger moving more anteriorly to the ANT-2 conditions. This occurs because, when subjected to the short duty cycles and long strains (which increase shortening deactivation; Rome and Swank, 1992) found in the POST position, the faster relaxation rate in ANT-1 muscle has less impact on power generation than in the short-strain, long-duty-cycle conditions found at the front of the fish. Under ANT-1 conditions, the level of power output is low in bundles from all positions; however, the difference in contractile properties can lead to substantial and even qualitative differences, e.g. the ANT-1 muscle generates positive work under ANT-1 conditions for 80 cm s^{-1} (6.4 Hz), while muscle from the more posterior positions cannot generate any power under the ANT-1 conditions (Fig. 7B, see also Fig. 3 in Rome et al., 1993).

The MID muscle generated the least power under most conditions, even smaller than the POST muscle (Tukey multiple-comparison test, $P<0.05$). The MID muscle does seem to have a slightly slower relaxation rate than the POST muscle (Fig. 2), but this difference is not statistically significant.

Overall, this analysis shows that the differences in *in vivo* conditions along the length of the fish are a more important determinant of power production than are the differences in contractile properties along the length of the fish.

Discussion

Our most perplexing finding is that the power output of red muscles driven under their measured *in vivo* conditions at 10 °C is far lower than we would predict on the basis of optimized work-loop experiments. This leads to an extremely

Table 1. *Results from the sensitivity analysis showing power generated by muscle bundles after small alterations from the measured* in vivo *conditions at 10 °C*

	ANT-1 (W kg^{-1})	ANT-2 (W kg^{-1})	MID (W kg^{-1})	POST (W kg^{-1})
Power at 30 cm s^{-1} (2.85 Hz)				
Measured	1.3±0.2 (6)	0.7±1.1 (6)	2.1±0.6 (6)	7.7±1.3 (9)
Long strain	1.2±0.2 (4)	−1.8±1.3 (4)	2.3±0.4 (4)	8.6±0.4 (6)
Phase early	NA	NA	1.8 (1)	8.9±0.2 (3)
Manual selection	1.3±0.3 (4)	0.5±1.2 (4)	2.7±0.2 (2)	7.9±0.3 (3)
Stim frequency	NA	NA	NA	7.2±1.8 (2)
Power at 40 cm s^{-1} (3.55 Hz)				
Measured	−2.4±0.4 (4)	−2.7±1.2 (5)	−1.3±0.4 (9)	3.4±0.8 (8)
Long strain	−3.8±0.6 (4)	−5.6±2.1 (3)	−0.3±0.6 (6)	4.1±1.1 (4)
Phase early	NA	NA	0.7±0.3 (2)	6.7±1.0 (2)
Manual selection	NA	−4.3±1.8 (2)	−0.6±0.9 (5)	3.9±0.3 (3)
Power at 50 cm s^{-1} (4.0 Hz)				
Measured	−3.1±0.9 (4)	−4.4±1.8 (3)	−2.1±0.5 (4)	1.8±0.6 (6)
Long strain	−5.6±0.6 (4)	−7.4±6.9 (2)	−2.9 (1)	3.1±0.6 (6)
Phase early	NA	NA	NA	4.8±0.6 (4)*
Manual selection	NA	NA	−2.2 (1)	2.4±0.2 (2)
Stim frequency	NA	NA	NA	1.6±0.2 (3)

The first row for each speed is power generated using the conditions measured in Swank and Rome (1999) for muscle from all four positions. Strain was increased 1.25-fold for long strain conditions, and phase was decreased by 15% (shifted earlier) for phase early conditions.

Manual selection conditions were found by remeasuring electromyogram (EMG) duration by rectifying the EMG trace, taking the derivative and excluding spikes at the start or end of EMGs that did not have steep slopes. The new duty cycles resulting from this are shown in Fig. 6. Note that this also results in a slight phase change.

In stimulation (Stim) frequency conditions, stimulation frequency was reduced to 57 Hz at 30 cm s^{-1} and to 50 Hz at 50 cm s^{-1}.

Values are means ± S.E.M., *N* is given in parentheses.

*A statistically significant difference from the measured value (*t*-test, $P<0.05$). NA, not tested.

Power was measured in W kg^{-1} muscle.

Details of the four positions, ANT-1, ANT-2, MID and POST, are given in the text.

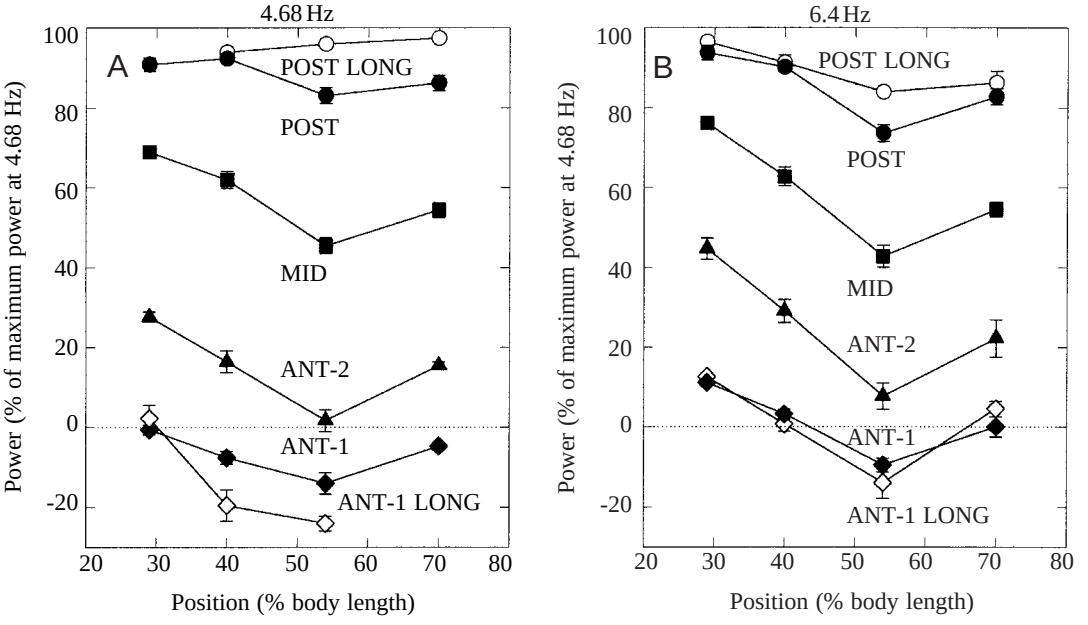

Fig. 7. Power generated by muscle bundles at 20 °C at each position when driven through *in vivo* conditions from all locations measured during swimming (see Swank and Rome, 1999). The position from which the muscle was dissected is shown by the placement along the *x*-axis. The various sets of *in vivo* conditions through which the muscles were driven are connected by lines and are marked next to each line. The differences in *in vivo* conditions with position have a greater effect on power generation than the differences in contractile properties, but the difference in relaxation rate (fastest at the ANT-1 position, slowest at the MID) also has a statistically significant effect on power-generating ability for all sets of conditions (one-way ANOVA, $P<0.001$ for all conditions at 6.4 Hz, P no greater than 0.013 for all conditions at 4.68 Hz). ANT-1 LONG (open diamonds) and POST LONG (open circles) conditions are identical to ANT-1 and POST conditions except that percentage strain was increased by 1 % of resting muscle length. Values are means ± S.E.M., N=4–8.

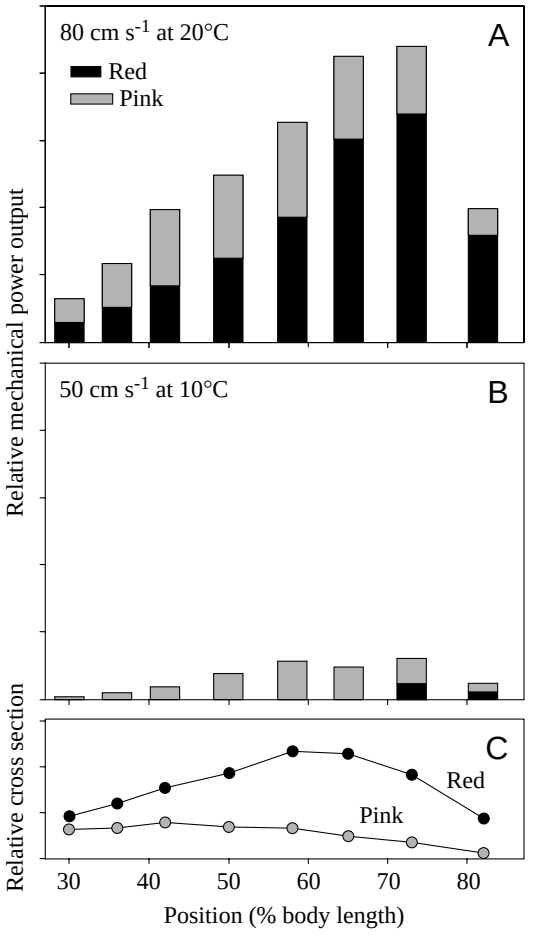

Fig. 8. Comparison of total power generated by scup red and pink musculature at the maximum sustainable swimming speeds at 20 °C (A) and 10 °C (B). The height of each column of the histogram corresponds to the power that the red (black) and pink (grey) musculature generates at that location (i.e. the product of muscle mass and mass-specific power production). Pink muscle data are from Coughlin and Rome (1996). Note that these pink muscle measurements were made on bundles taken exclusively from the ANT-2 position (40 % body length) because it is not possible to obtain pure pink muscle bundles from other positions. Note also that the *in vivo* conditions for the POST position (70 % body length) were approximated to those of the red muscle at this position because there was not sufficient pink muscle at the POST position from which to record electromyograms. (C) The relative cross section of the red and pink muscle along the length of the fish (data from Zhang et al., 1996).

high and sometimes indeterminate Q_{10} value in anterior regions of the fish. In addition, our sensitivity analysis strongly suggests that this is not due to random or systematic errors in the measurement of *in vivo* parameters through which the muscle is driven. So how do fish power steady swimming at low temperatures? Below, we describe some additional analyses performed to address power generation during swimming at low temperatures. We also discuss the implications of our findings on general methodologies used to study the effects of temperature on the biomechanics of locomotion.

Power output of the red muscle at different temperatures

The low power generated per kilogram of red muscle during swimming at 40 and 50 cm s^{-1} at 10 °C is striking. To assess better the effects of temperature on overall power generation during swimming at these speeds, we obtained the relative power generated by the red musculature by integrating along the body of the fish the product of power per kilogram and red muscle mass at each position. The quantitative distribution of muscle fibre types along the length of scup has been described previously (Zhang et al., 1996). In this calculation, we assumed that no section of the fish generates negative work. Clearly, at 40 and 50 cm s^{-1} at 10 °C, the net power output per kilogram of muscle in ANT-1, ANT-2 and MID positions is negative. In the worst case, this negative work could more than cancel out any positive power production in the POST region of the fish. Thus, to try to determine the maximum power the red muscle could generate, we set negative values to zero with the assumption that, if muscle fibres in these positions are generating negative work, they would not be heavily recruited. By setting the total power output of the red musculature while swimming at 80 cm s^{-1} at 20 °C to a value of 1, we calculate the following relative power outputs: 1.02 at 50 cm s^{-1} at 20 °C, 0.03 at 50 cm s^{-1} at 10 °C, 0.056 at 40 cm s^{-1} at 10 °C and 0.25 at 30 cm s^{-1} at 10 °C.

By comparing these values with the approximate relative power required for swimming, it seems unlikely that scup can power swimming at 50 or even 40 cm s^{-1} at 10 °C using their red muscle alone. For this comparison, we assume that the power required for swimming increases with swimming speed with an exponent of 2.5–3.0 (Webb, 1978). We also assumed that the red muscle is maximally recruited at the maximum swimming speed at which fish can swim without recruiting their white muscle (80 cm s^{-1} at 20 °C).

At 50 cm s^{-1} at 10 °C, the fish's red musculature would generate only approximately 3 % of the power generated at 80 cm s^{-1} at 20 °C. Yet, to swim at 50 cm s^{-1}, the fish needs to generate approximately 24–31 % of the power required at 80 cm s^{-1}. This discrepancy suggests that it is unlikely that the red muscle could be generating all the power required for swimming at 50 cm s^{-1} at 10 °C. Similarly, at 40 cm s^{-1}, the muscle generates only approximately 6 % of the power at 80 cm s^{-1}, which is still substantially below the approximately 12–18 % required for swimming at this speed. This discrepancy suggests that the red muscle could not power swimming at 40 cm s^{-1} either. In contrast, at 30 cm s^{-1}, the fish needs to generate only approximately 5–9 % of the power needed at 80 cm s^{-1}, yet if the muscle were fully recruited it could generate 25 % of the power the red muscle generates at 80 cm s^{-1} at 20 °C. This suggests that the fish would be capable of swimming at this speed at 10 °C using its red muscle alone.

Pink muscle plays a crucial role in powering swimming at low temperature

Given the apparent inability of the red muscle to power swimming at moderate speeds (40–50 cm s^{-1}) at 10 °C where the white muscle is not recruited, coupled with the recent data

on pink muscle fibre recruitment (Coughlin and Rome, 1999) and power production (Coughlin and Rome, 1996; Coughlin et al., 1996b), it is likely that pink muscle plays an important role in powering steady swimming at low temperatures. Pink muscle forms a thin muscle mass running longitudinally medial to the red muscle. Scup pink muscle has been found to have much faster contraction kinetics than red muscle, which appears to be crucial for power generation at low temperatures. In particular, at 10 °C, pink muscle activates and relaxes approximately twice as quickly as red muscle and has an approximately 1.5-fold higher V_{max} (Coughlin et al., 1996b). This translates into a 1.5-fold higher power output during optimized work-loop experiments and an approximately 1.5-fold shift to higher frequencies at which the optimum is achieved (f_{opt}) (Coughlin et al., 1996b).

Recently, Coughlin and Rome (1996) measured the approximate *in vivo* conditions for pink muscle during swimming at 50 cm s^{-1} at 10 °C and 80 cm s^{-1} at 20 °C, and measured pink muscle power output while driven through their *in vivo* conditions (see legend to Fig. 8 for details). These data show that the pink muscle is capable of generating far more mechanical power under *in vivo* conditions at 10 °C than can the red muscle. Whereas the red muscle could generate net positive power in only the POST position at 50 cm s^{-1} at 10 °C, the pink muscle could generate positive power in all positions. To assess the effects of pink muscle on the relative power production of the total musculature, the product of power output per kilogram of pink muscle and pink muscle mass at each position was also integrated along the length of the fish (Fig. 8A,B). Strikingly, despite the fact that pink muscle has only one-third the mass of red muscle, during swimming at 50 cm s^{-1} at 10 °C, the pink muscle is capable of generating approximately six times more power than the red muscle (Fig. 8B). At 80 cm s^{-1} at 20 °C (Fig. 8A), the pink muscle generates only approximately 50 % of the power generated by the red muscle (reflecting the pink muscle's much lower volume, see Fig. 8C). Taking into account the contribution of the pink muscle, the aerobic musculature (red and pink) at 50 cm s^{-1} at 10 °C can generate approximately 20 % and 15 % of the power generated at 80 cm s^{-1} (20 °C) by the red muscle (alone) and the aerobic muscle, respectively. Although not matching the power required perfectly, it appears close at this level of approximation.

Although these *relative* comparisons are useful, it is clear that far stronger arguments could be made with accurate measures (or calculations) of the power required for swimming at different speeds. More *absolute* assessments of what speeds could be powered by the muscle types could then be made.

Because the pink muscle plays such an important role in powering swimming at low temperatures and the pink muscle is distributed more anteriorly than the red (Fig. 8C and Zhang et al., 1996), it is useful to consider how the inclusion of pink muscle affects the distribution of power production along the length of the fish. As can be seen in Fig. 8, power generation is somewhat more evenly distributed along the fish at low temperatures than at high temperatures. Nonetheless, most of the power is generated in the posterior half of the fish and relatively little in the anterior part of the fish. This reflects both the low power output per kilogram of muscle in the anterior (due to the low strain and long stimulation duration) and the small muscle mass of red muscle in the anterior.

The influence of temperature on power production in vivo

The case of scup red muscle is a clear example of the limitations of predicting whole-animal function from Q_{10} values of isolated tissue and of the care necessary to understand the effects of temperature on the whole animal. For scup red muscle, temperature has markedly different effects on power production depending on the conditions examined. For instance, in scup red muscle at 10 °C and 20 °C, power output has a Q_{10} of 1.8 during steady-state force–velocity measurements (Rome et al., 1992b). In 'optimized' oscillatory contractions (where length change and stimulation conditions are systematically varied), the Q_{10} for power generation is approximately 2.3 (Rome and Swank, 1992), which is a fairly typical value (Stevenson and Josephson, 1990; Swoap et al., 1993; Altringham and Block, 1997). When examined at a *given* oscillation frequency (with the length and stimulation parameters optimized for that frequency), the Q_{10} for power production increases with increasing oscillation frequency. Over the range of frequencies used by scup during swimming, the Q_{10} increases from approximately 3 to approximately 5 (Rome and Swank, 1992).

When muscles are driven under *in vivo* conditions, the Q_{10} becomes even larger. Because the *in vivo* conditions are much further from the 'optimized' conditions at a given frequency at low temperatures (Fig. 6), the *in vivo* power is disproportionately reduced at low temperatures. For the POST position, the Q_{10} for power production varies between 4 and 14 depending on speed. However, for more anterior positions in the fish, power production is so reduced in many of the *in vivo* conditions examined (i.e. the ANT-1, ANT-2 and MID positions at 40 and 50 cm s^{-1} at 10 °C) that the red muscle generates no net power (i.e. net power production is negative). In the case where net power production is zero or negative, the Q_{10} becomes indeterminate. Thus, for the ANT-1, ANT-2 and MID positions, the Q_{10} for power production is large and essentially indeterminate.

The preceding analysis necessitates a re-evaluation of how temperature effects in general, and particularly those on muscle, are addressed. Historically, scientists have compared Q_{10} values of certain variables of isolated tissues or enzymes and have tried to relate these Q_{10} values to those of organismal function (for reviews, see Rome, 1990, 1998). In the light of the present findings, this approach seems over-simplified and in some cases may be inappropriate. Although isolated muscle run under optimized conditions may have a normal Q_{10} (1.5–2.5), these temperature effects may be so significantly altered when muscles are working under *in vivo* conditions that conclusions based on Q_{10} values from maximal or optimized conditions may be qualitatively incorrect. To make a meaningful assessment of the effects of temperature on muscle performance during swimming or to appreciate muscle design,

muscle performance must be studied under the conditions in which the muscle operates *in vivo*.

Power production along the length of the fish: a general approach for studying muscle function during locomotion

One of the fundamental questions of fish biomechanics is where along the length of the fish is the power generated for swimming? Whereas we (Rome et al., 1993; present study), as well as Johnson et al., (1994), have found that most of the power during steady sustainable swimming is generated in the posterior region of the fish, Hess and Videler (1984), van Leeuwen et al. (1990), van Leeuwen (1995) and Altringham et al. (1993) have suggested that much of the power is generated in the anterior portion and may be transmitted through the posterior region to the tail. In a review, Wardle et al. (1995) have suggested that the different conclusions might reflect fundamental differences in how various species swim. For instance, Wardle et al. (1995) suggested that scup swimming differs from that of other species in that the wavelength of the bending wave (λ_B) greatly exceeds the length of the fish's body: they determined λ_B of scup to be 1.54 compared with values of 1.0 for mackerel *Scomber scombrus* and saithe *Pollachius virens*, and 1.25 for carp *Cyprinus carpio*. However, in more detailed studies, Swank and Rome (1999) showed that, although at the top sustainable swimming speed in scup the value exceeds 1 (it is 1.34), at more moderate speeds it is approximately equal to 1 (see Fig. 1C in Swank and Rome, 1999). Thus, over most swimming speeds, scup have a λ_B quite similar to those reported for other fish, suggesting that differences in λ_B probably do not underlie the differences in conclusions concerning the location of power generation.

However, differences in the methodologies employed may also be responsible for differing conclusions. During work-loop experiments, muscles function like an analog computer. Muscles produce a complex operation on the inputs (length-change amplitude, shape of the length change, oscillation frequency, stimulation duration, stimulation phase and stimulus waveform). The outputs (force and power) clearly depend on the inputs (see Figs 4, 5).

Hence, accurate determination of how power is generated in a given species of fish requires highly accurate input information. Our laboratory has adopted several procedures to obtain accurate information for scup. We have determined the muscle length changes in three ways: (1) calculation from the curvature of the backbone using beam theory (Rome et al., 1988); (2) calculation from an empirical equation relating sarcomere length measured in frozen sections to backbone curvature (Rome and Sosnicki, 1991; Rome et al., 1992a), and (3) using sonomicrometry (Coughlin et al., 1996a). All these techniques agree closely in terms of amplitude and phase. This is important because Katz et al. (1999) suggested that a different method of measuring strain (used in the past by others) may have introduced a phase error leading to a misinterpretation of power production. Further, we have developed new techniques to provide highly accurate synchronization between film and EMG recordings (Rome, 1995) and have developed techniques to ensure that muscle strain and EMGs are measured at precisely the same position on the fish. Finally, we have obtained EMGs with a high signal-to-noise ratio and have used computer analysis to improve our determination of EMG onset and offset times.

A second procedure that we believe is required to help obtain reasonable answers is sensitivity analysis, such as that described in the present study (see also Full et al., 1998). As mentioned above, the muscle produces a complex operation on the inputs which may be nonlinear. Hence, relatively small systematic errors could, in theory, result in large changes in power output. As mentioned above and in Swank and Rome (1999), overfiltering length recordings could potentially have led to reduced amplitude. More importantly, the criteria for the EMG onset and offset times are necessarily arbitrary, and this can lead to unavoidable uncertainties about the stimulation pattern. Thus, we believe a second necessary part of this overall procedure is the performance of a sensitivity analysis to test specifically whether random or systematic errors in the measurement of *in vivo* parameters could lead to major differences in our conclusions about power output.

We also believe that the combination of accurate *in vivo* information and the work-loop technique makes it possible to determine whether differences in the distribution of power generation among species, should they exist, are due to differences in the *in vivo* length-change and stimulation patterns or to differences in the contractile properties of the muscle itself. For instance, by using the procedure of driving muscles from the ANT-1 and POST positions through the *in vivo* conditions measured from both the ANT-1 and POST positions, we showed that the low power output of the ANT-1 muscle during swimming was not due to insufficiency of its contractile properties, but rather to non-optimality of its *in vivo* parameters. By analogy, this approach can be applied to different species. Muscle from one species can be driven under the length-change and stimulation pattern of another species and the resulting power measured. By doing so, we should gain insight into whether the contractile properties of the muscle or the *in vivo* length change and stimulation pattern are ultimately responsible for differences in power production.

We dedicate this series of papers to the memory of Frank Carey. Frank was a long-time mentor, friend and inspiration who sparked in L.C.R. a career-long interest in temperature, muscle and fish swimming. We thank Dr Iain Young for critically reviewing the manuscripts. Supported by NIH AR38404, NIH AR46125 and NSF IBN-9514383 and by the University of Pennsylvania Research Foundation.

References

Altringham, J. D. and Block, B. (1997). Why do tuna maintain elevated slow muscle temperatures? Power output of muscle isolated from endothermic and ectothermic fish. *J. Exp. Biol.* **200**, 2617–2627.

Altringham, J. D. and Johnston, I. A. (1990). Modelling muscle power output in a swimming fish. *J. Exp. Biol.* **148**, 395–402.

Altringham, J. D., Wardle, C. S. and Smith, C. I. (1993). Myotomal muscle function at different locations in the body of a swimming fish. *J. Exp. Biol.* **182**, 191–206.

Coughlin, D. J. and Rome, L. C. (1996). The role of pink and red muscle in powering steady swimming in scup, *Stenotomus chrysops*. *Am. Zool.* **36**, 666–677.

Coughlin, D. J. and Rome, L. C. (1999). Muscle activity in steady swimming scup, *Stenotomus chrysops* is a function of fiber type and body position. *Biol. Bull.* **196**, 145–152.

Coughlin, D. J., Valdes, L. and Rome, L. C. (1996a). Muscle length changes during fish swimming: a comparison of sonomicrometry and anatomical-high speed ciné techniques. *J. Exp. Biol.* **199**, 459–463.

Coughlin, D. J., Zhang, G. and Rome, L. C. (1996b). Contractile dynamics and power production of pink muscle of the scup. *J. Exp. Biol.* **199**, 2703–2712.

Davies, M. L. and Johnston, I. A. (1995). Muscle fibers in rostral and caudal myotomes of the Atlantic cod (*Gadus morhua* L.) have different mechanical properties. *Physiol. Zool.* **68**, 673–697.

Full, R. J., Stokes, D. R., Ahn, A. N. and Josephson, R. K. (1998). Energy absorption during running by leg muscles in a cockroach. *J. Exp. Biol.* **201**, 997–1012.

Hess, F. and Videler, J. J. (1984). Fast continuous swimming of saithe (*Pollachius virens*): a dynamic analysis of bending moments and muscle power. *J. Exp. Biol.* **109**, 229–251.

Johnson, T. P., Syme, D. A., Jayne, B. C., Lauder, G. V. and Bennett, A. F. (1994). Modeling red muscle power output during steady and unsteady swimming in largemouth bass. *Am. J. Physiol.* **267**, R481–R488.

Josephson, R. K. (1985). Mechanical power output from striated muscle during cyclic contraction. *J. Exp. Biol.* **114**, 493–512.

Josephson, R. K. and Stokes, D. R. (1989). Strain, muscle length and work output in crab muscle. *J. Exp. Biol.* **145**, 45–61.

Katz, S. L., Shadwick, R. E. and Rapoport, H. S. (1999). Muscle strain histories in swimming milkfish in steady and sprinting gaits. *J. Exp. Biol.* **202**, 529–541.

Marsh, R. L. (1990). Deactivation rate and shortening velocity as determinants of contractile frequency. *Am. J. Physiol.* **259**, R223–R230.

Marsh, R. L., Olson, J. M. and Guzik, S. K. (1992). Mechanical performance of scallop adductor muscle during swimming. *Nature* **357**, 411–413.

Rome, L. C. (1990). The influence of temperature on muscle recruitment and function *in vivo*. *Am. J. Physiol.* **259**, R210–R222.

Rome, L. C. (1995). A device for synchronizing physiological data to cine film. *J. Biomech.* **28**, 333–338.

Rome, L. C. (1998). Some advances in integrative muscle physiology. *Comp. Biochem. Physiol.* **120**, 51–72.

Rome, L. C., Choi, I., Lutz, G. and Sosnicki, A. A. (1992a). The influence of temperature on muscle function in fast swimming scup. I. Shortening velocity and muscle recruitment during swimming. *J. Exp. Biol.* **163**, 259–279.

Rome, L. C., Funke, R. P., Alexander, R. McN., Lutz, G., Aldridge, H. D. J. N., Scott, F. and Freadman, M. (1988). Why animals have different muscle fibre types. *Nature* **355**, 824–827.

Rome, L. C. and Sosnicki, A. A. (1990). The influence of temperature on mechanics of red muscle in carp. *J. Physiol., Lond.* **427**, 151–169.

Rome, L. C. and Sosnicki, A. A. (1991). Myofilament overlap in swimming carp. II. Sarcomere length changes during swimming. *Am. J. Physiol.* **260**, C289–C296.

Rome, L. C., Sosnicki, A. A. and Choi, I. (1992b). The influence of temperature on muscle function in the fast swimming scup. II. The mechanics of red muscle. *J. Exp. Biol.* **163**, 281–295.

Rome, L. C. and Swank, D. (1992). The influence of temperature on power output of scup red muscle during cyclical length changes. *J. Exp. Biol.* **171**, 261–281.

Rome, L. C., Swank, D. and Corda, D. (1993). How fish power swimming. *Science* **261**, 340–343.

Stevenson, R. D. and Josephson, R. K. (1990). Effects of operating frequency and temperature on mechanical power output from moth flight muscle. *J. Exp. Biol.* **149**, 61–78.

Swank, D. and Rome, L. C. (2000). The influence of temperature on power production during swimming. I. *In vivo* length change and stimulation pattern. *J. Exp. Biol.* **203**, 321–331.

Swank, D., Zhang, G. and Rome, L. C. (1997). Contraction kinetics of red muscle in scup: mechanism for variation in relaxation rate. *J. Exp. Biol.* **200**, 1297–1307.

Swoap, S. J., Johnson, T. P., Josephson, R. K. and Bennett, A. F. (1993). Temperature, muscle power output and limitations on burst locomotory performance of the lizard *Dipsosaurus dorsalis*. *J. Exp. Biol.* **174**, 185–197.

van Leeuwen, J. L. (1995). The action of muscles in swimming fish. *Exp. Zool.* **80**, 177–191.

van Leeuwen, J. L., Lankheet, M. J. M., Akster, H. A. and Osse, J. W. M. (1990). Function of red axial muscle of carp (*Cyprinus carpio* L.): recruitment and normalised power output during swimming in different modes. *J. Zool., Lond.* **220**, 123–145.

Wardle, C. S., Videler, J. J. and Altringham, J. D. (1995). Tuning in to fish swimming waves: body form, swimming mode and muscle function. *J. Exp. Biol.* **198**, 1629–1636.

Webb, P. W. (1978). Hydrodynamics: non-scombroid fish. In *Fish Physiology*, vol. 7 (ed. W. S. Hoar and D. J. Randall), pp. 189–237. New York: Academic Press.

Zhang, G., Swank, D. and Rome, L. C. (1996). Quantitative distribution of muscle fiber types in the scup. *J. Morph.* **29**, 71–81.